ELSEVIER

Journal of Photochemistry and Photobiology A: Chemistry 123 (1999) 53–59

Journal of Photochemistry and Photobiology A:Chemistry

Solvent effects on rates of photochemical reactions of rose bengal triplet state studied by nanosecond laser photolysis

Shafiqul D.-M. Islam, Osamu Ito*

Institute for Chemical Reaction Science, Tohoku University, Katahira, Aoba-ku, Sendai 980-8577, Japan

Received 16 November 1998; received in revised form 7 January 1999; accepted 16 February 1999

Abstract

Bimolecular rate constants of energy transfer, electron-transfer, and H-atom abstraction reaction have been determined by following the transient absorption bands of the triplet states of rose bengal [$^3(RB^{2-})^*$] at about 1020 nm with various substrates using nanosecond laser flash photolysis. For electron acceptor (1,4-benzoquinone), electron-transfer takes place via an exciplex. Exciplex formation was found to be predominant in high viscosity solvents rather than low viscosity solvents. For electron donor (3,3′,5,5′-tetramethylbenzidine), the rate constants are independent of solvent viscosity, indicating that the contribution to an exciplex formation is small. The H-atom abstraction reactions of $^3(RB^{2-})^*$ with H-donors show that the rate constants in water are higher than those in ethanol and in THF. The negative slopes of the Hammett plots indicate that the reaction center of [$^3(RB^{2-})^*$] has a highly electrophilic nature, which increases with solvent polarity, suggesting the polar transition states. © 1999 Elsevier Science S.A. All rights reserved.

Keywords: Solvent effects; Rose bengal; Laser photolysis; Energy transfer; Electron transfer; Hydrogen abstraction; Triplet; Exciplex

1. Introduction

Xanthene dyes have been widely studied for their promising sensitizers for the photochemical reactions in various solvents [1–12]. Particularly, heavy atom-substituted xanthene dyes such as rose bengal (RB^{2-}) are notable for their high triplet quantum yields (Φ_T = ca. 1) and for fairly long lived triplet states ($t_{1/2} = 0.1$–0.3 ms) [10]. As a result of its photophysical and photochemical properties, RB^{2-} is well-established as a sensitizer in photography [13,14], in singlet-oxygen ($^1O_2$) formation and in the oxidation of biological important molecules [15]. The triplet state of RB^{2-}[$^3(RB^{2-})^*$] participates in energy-transfer, electron-transfer and H-atom abstraction reactions.

The energy of $^3(RB^{2-})^*$ determined from phosphorescence measurements (1.77 eV) [16,17] is sufficiently high to transfer triplet energy to molecules with a lower triplet energy such as anthracene derivatives and β-carotene. There have been a number of studies on electron transfer reaction of $^3(RB^{2-})^*$ [10,18,19]; both oxidative and reductive quenching reactions are thermodynamically favorable with many electron donors and acceptors [10,18,19]. H-abstraction reactions of $^3(RB^{2-})^*$ have also been studied with different quenchers [8,11,20,21]. In general, the electron transfer reactions depend on the polarity and viscosity of the solvents. It is known that the H-abstraction reactions of aromatic carbonyl triplet states depend on solvent polarity and substituents which affect the electronic character of the lowest triplet state [22–24].

In the previous paper [25], we described that the triplet states of xanthene dyes such as eosine and erythrosine showed the intense transient absorption bands in the near-IR region in addition to the weak one in the visible region (ca. 600 nm). In the present paper, we have studied extensively the reactivities of ($^3RB^{2-})^*$ in various solvents in order to make clear the solvent dependence of the rates for various reactions [26–28]. A particular focus has been directed to both electron transfer and H-abstraction reactivity of $^3(RB^{2-})^*$ in various solvents. Thus, the elemental reaction processes have been confirmed by direct observation of the decay of ($^3RB^{2-})^*$ and the rise of ion radicals or free radicals.

2. Experimental

Rose bengal (RB^{2-}) with purity greater than 99% was commercially supplied. The quenchers were all commercially available. Most of the reagents were purified by recrystallization or distillation.

---

*Corresponding author. Tel.: +81-22-227-6200; fax: +81-22-217-5608; e-mail: ito@icrs.tohoku.ac.jp

1010-6030/99/$ – see front matter © 1999 Elsevier Science S.A. All rights reserved.
PII: S1010-6030(99)00042-8

The solutions containing RB^{2-} and quenchers were excited by 532 nm light from a Nd:YAG laser (6 ns fwhm) with 7–10 mJ power. For measurements of the transient absorption spectra in the visible region, a photomultiplier was used as a detector for monitoring the transmitted light from a continuous Xe-monitor lamp (150 W). In the near-IR region, a Ge-APD detector and a pulsed xenon-monitoring lamp were employed [29]. The steady-state UV/VIS absorption spectra were measured with a JASCO/V-570 spectrophotometer. All measurements were performed at 23°C.

3. Results and discussion

3.1. Steady-state spectra

The steady-state absorption spectra of RB^{2-} in different solvents are shown in Fig. 1. The main absorption peak (λ_{max}) appears at 543–552 nm with a shoulder at 500–520 nm. With decreasing the solvent polarity, the λ_{max} shifts to longer wavelength up to 553 nm in DMF, excepting water. The λ_{max} in aqueous solution is shorter wavelength compared to those in other solvents, suggesting a strong hydrogen bond between the solvent and RB^{2-}. The molar extinction coefficients (ϵ) are in the range of (3.6–10.6) $\times 10^4\,M^{-1}\,cm^{-1}$. The relative intensity of the shoulder to the peak may be a measure of aggregation in RB^{2-} [30]. In most solvents, the ratios are in the range of 0.32–0.38, while the ratio in tetrahydrofuran (THF) is the highest (0.48), suggesting some aggregations. In water, since the ratio is slightly high (0.42), a weak interaction has to be taken into consideration. Similar tendencies are reported for the fluorescence maxima of xanthene dyes [31].

3.2. Transient absorption spectra

RB^{2-} can be excited by 532 nm laser light due to its intense absorption at this wavelength. Fig. 2 shows the transient absorption spectra observed following 532 nm-laser excitation of RB^{2-} in ethanol. The absorption band with a peak at 1020 nm appears immediately after the nanosecond laser pulse. This absorption band in the region of 600–1350 nm with a peak at 1020 nm was attributed to T–T absorption band by its similarity with the reported T–T absorption bands of other xanthene dyes such as fluorescein, eosine and erythrosine [32,33]. The λ_{max} of the transient spectrum of $^3(RB^{2-})^*$ in acetonitrile and THF is slightly blue-shifted compared to water. The intensity of the transient absorption of $^3(RB^{2-})^*$ in THF also decreased compared to other solvents; this tendency is similar as the steady-state absorption in THF.

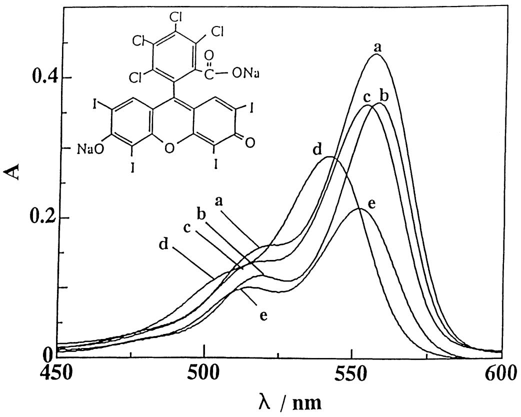

Fig. 1. Steady-state absorption of RB^{2-} (2.0×10^{-5} M, cell = 2 mm) in various solvents; (a) acetone, (b) 1-butanol, (c) ethanol, (d) water, (e) THF.

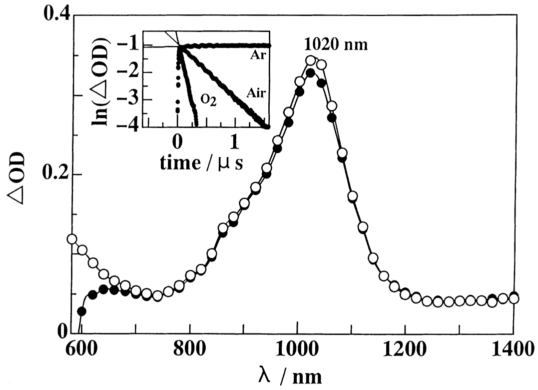

Fig. 2. Transient absorption spectra observed after 532 nm laser pulsing of RB^{2-} (2.0×10^{-5} M) in deaerated ethanol at 0.1 μs (●) and 1 μs (○). Insert: decay profiles of the T–T absorption band at 1020 nm.

3.3. Quenching with O_2 and other triplet quenchers

$^3(RB^{2-})^*$ was effectively quenched by O_2 as shown in the inset to Fig. 2, in which the decay time-profiles were converted into first-order plots. From the slope of the linear plots, the first-order rate constant (k_{1st}^{obs}) was evaluated. The second-order rate constant for O_2-quenching reaction (k_{O_2}) was obtained from the pseudo-first-order plot (k_{1st}^{obs} versus $[O_2]$) as listed in Table 1. For O_2-quenching reaction, both energy transfer and electron transfer can be considered, producing singlet oxygen ($^1O_2$) and superoxide radical

Table 1
Second-order rate constants for the quenching of $^3(RB^{2-})^*$ with triplet quenchers (k_q)

Sensitizer/quencher	Solvent	k_q ($M^{-1}\,s^{-1}$)	T_1[a] (eV)
Thioxanthone	AN[b]	9.0×10^9	2.82
Rose Bengal		–	1.77
ZnTPP	Ethanol	5.9×10^8	1.59
Methylene blue	Ethanol	7.4×10^9	1.50
O_2	Ethanol	9.0×10^8	1.09
	Water	1.5×10^9	
	THF[c]	7.3×10^8	

[a] T_1 values were cited from references [5,16,17,39–42].
[b] AN – acetonitrile.
[c] THF – tetrahydrofuran.

ion ($O_2^{\bullet -}$) as Equations 1 and 2, respectively, in polar solvents [34–36]. In the present study, the half-oxidized form of RB^{2-} is represented as $(RB^{2-})^{\bullet +}$, but not $RB^{\bullet -}$, because the two negative charges of RB^{2-} are localized at the two O-atoms, while the cation radical may be delocalized on the π-orbitals of molecule. It has been reported that the quantum yield of $^1O_2$ formation for RB^{2-} is 0.76–0.86 in polar solvents [37,38]. Thus, energy transfer is predominant to the electron transfer producing $O_2^{\bullet -}$. It is notable that the k_q values of $^3(RB^{2-})^*$ with O_2 increase with solvent polarity (Table 1).

$$^3(RB^{2-})^* + O_2 \xrightarrow{k_{O_2}} \begin{cases} (RB^{2-}) + {}^1O_2 & (1) \\ (RB^{2-})^{\bullet +} + O_2^{\bullet -} & (2) \end{cases}$$

For dyes with low T_1 energy such as methylene blue and zinc tetraphenylporphirin (ZnTPP), the energy transfer rate constants (k_{ent}) were evaluated as listed in Table 1, in which the value for methylene blue is close to diffusion controlled limit (k_{diff}), while that for ZnTPP is ca. 1/10 of k_{diff}. The higher k_{ent} values for methylene blue than that of ZnTPP may be expected due to the interaction $^3(RB^{2-})^*$ with methylene blue.

Sensitization of $^3(RB^{2-})^*$ was found when thioxanthone (TXO) was excited in the presence of RB^{2-} with THG (355 nm) light, which predominantly excites TXO accompanied by slight excitation of RB^{2-} due to its weak absorption at this wavelength. The transient absorption bands at 620 nm and 1020 nm were attributed to T–T absorption bands of $^3TXO^*$ [43,44] and $^3(RB^{2-})^*$, respectively (Fig. 3). The inserted time-profiles in Fig. 3 show the decay of $^3TXO^*$ and rise of $^3(RB^{2-})$, indicating that energy transfer occurs from $^3TXO^*$ to RB^{2-}. The initial rise of $^3(RB^{2-})^*$ was attributed to the direct excitation of RB^{2-}.

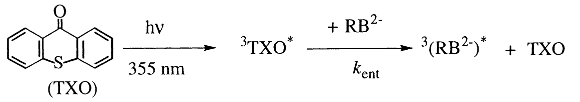

(3)

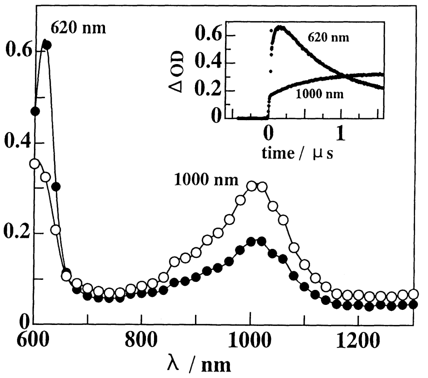

Fig. 3. Transient absorption spectra observed after 355 nm laser pulsing of thioxanthone (1.0×10^{-5} M) in the presence of RB^{2-} (6.0×10^{-5} M) at 0.1 μs (●) and 1 μs (○) in Ar-saturated AN. Insert: time-profiles at 620 nm and 1000 nm.

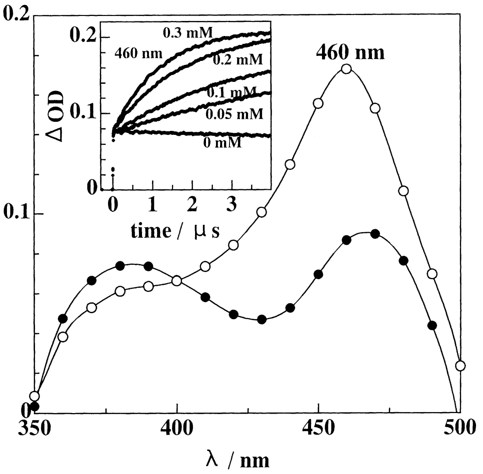

Fig. 4. Transient absorption spectra observed after 532 nm laser pulsing of RB^{2-} (2.0×10^{-5} M) in the presence of 1,4-benzoquinone (BQ) (3.0×10^{-4} M) in deaerated ethanol at 0.25 μs (●) and 2.5 μs (○). Insert: time profiles of $BQ^{\bullet -}$ at 460 nm.

From the decay rate of $^3TXO^*$ on adding RB^{2-}, k_{ent} for $^3(RB^{2-})^*$ was found to be $9.0 \times 10^9\ M^{-1}\ s^{-1}$ in acetonitrile, which is close to the diffusion-controlled rate constant. From Fig. 3, the molar extinction coefficient (ϵ_T) of $^3(RB^{2-})^*$ can be evaluated by comparison with the initial absorbance and ϵ_T for $^3TXO^*$, assuming that the quantum yield of energy transfer is equal to unity; thus, ϵ_T of $^3(RB^{2-})^*$ was found to be $13\,000\ M^{-1}\ cm^{-1}$ at 1020 nm.

3.4. Electron transfer to acceptor

In the presence of 1,4-benzoquinone (BQ), the transient absorption bands characteristic to the radical anion of BQ ($BQ^{\bullet -}$) appeared at 460 nm [11,44] with the decay of $^3(RB^{2-})^*$ at 1020 nm indicating that electron transfer occurs from $^3(RB^{2-})^*$ to BQ (Fig. 4). The inserted time-profiles in Fig. 4 show the rises of $BQ^{\bullet -}$ at various concentration of BQ. The transient absorption band of $(RB^{2-})^{\bullet +}$ at 460 nm may overlap with the absorption of $BQ^{\bullet -}$ at this wavelength [12]. The transient absorption band of $(RB^{2-})^{\bullet +}$ was confirmed by electron transfer from $^3(RB^{2-})^*$ to *p*-dinitrobenzene (DNB) in ethanol by observing the transient absorption bands of $(RB^{2-})^{\bullet +}$ at 460 nm and $DNB^{\bullet -}$ at ca. 900 nm.

Electron transfer for $^3(RB^{2-})^*$ with BQ was studied in various solvents with changing polarity and viscosity; the values of the rate constants (k_q) are listed in Table 2. These rate constants are obtained from a plot of the pseudo-first-order decay rate constants for $^3(RB^{2-})^*$ as a function of [BQ] in the low concentration range. The rates are dependent on viscosity of solvents (η) rather than dielectric constant. With increase in viscosity, the k_q values decrease from $8.6 \times 10^9\ M^{-1}\ s^{-1}$ in acetone to $1.8 \times 10^9\ M^{-1}\ s^{-1}$ in 1-butanol. In Fig. 5, the log k_q and log k_{diff} are plotted with log η [45] according to

Table 2
Second-order rate constants for the quenching of $^3(RB^{2-})^*$ with 1,4-benzoquinone (BQ) and TMB (k_q)

Solvent	Viscosity (cP)	k_q (M^{-1} s^{-1})	
		BQ	TMB
AN	0.345	7.1×10^9	1.2×10^9
THF	0.550	4.1×10^9	1.8×10^9
Acetone	0.304	8.6×10^9	9.2×10^8
DMF[a]	0.924	3.4×10^9	5.8×10^8
Water	1.002	3.7×10^9	–[b]
Ethanol	1.078	3.6×10^9	1.7×10^9
BN[c]	1.240	2.7×10^9	5.6×10^8
DMSO[d]	1.996	2.4×10^9	5.7×10^8
1-butanol	2.948	1.8×10^9	9.5×10^8

[a] DMF – N,N-dimethylformamide.
[b] TMB is not soluble in water.
[c] BN – benzonitrile.
[d] DMSO – dimethyl sulfoxide.

$$k_q = A\eta^{-\alpha} \tag{4}$$

where α is the viscosity dependency. Values for α ranging from zero to unity have been reported [46] for a number of bimolecular chemical reactions. From the slope for k_{diff}, $\alpha = 1$, whereas for BQ, $\alpha = 0.6$. This implies that the k_q values for BQ are considerably diffusion dependent. The k_q values are very close to k_{diff} values in high viscosity solvents, while the k_q values in low viscosity solvents are smaller than k_{diff}. In high viscosity solvents, the exciplex is presumed to be long lifetime. In low viscosity solvents, on the other hand, the lifetime of exciplex may be low. In general, electron transfer may take place on the basis of the free energy change of the reaction (ΔG°), which can be evaluated by the oxidation and reduction potentials and energy of excited state in adding solvation energy by using Rehm–Weller equation [47]. In the case of $^3(RB^{2-})^*$ and BQ, ΔG was evaluated to be -0.35 eV in ethanol and -0.48 eV in acetonitrile which may predict slightly lower electron transfer rate than k_{diff}.

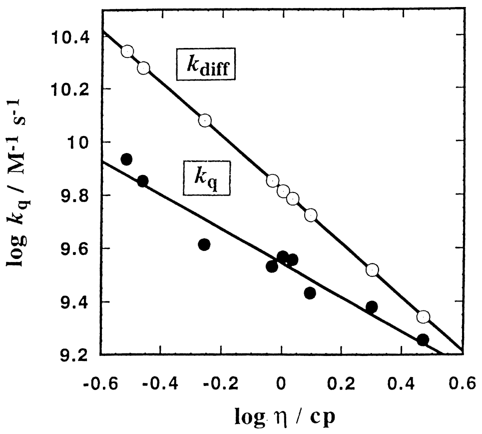

Fig. 5. Variation of bimolecular rate constants (log k_q) as a function of the solvent viscosity (log k_q) for $^3(RB^{2-})^*$-BQ system in various solvents.

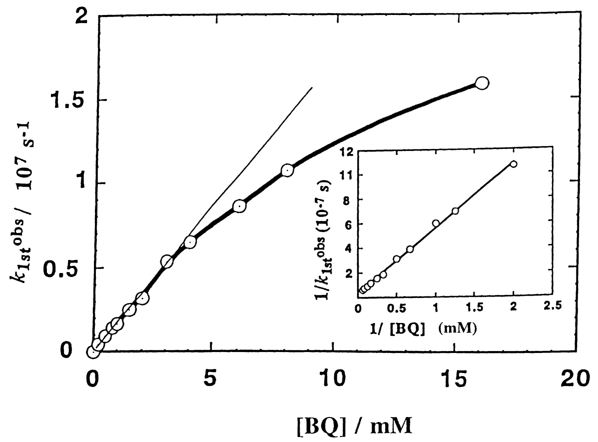

Fig. 6. First-order decay rate constants (k_{1st}^{obs}) of $^3(RB^{2-})^*$ in 1-butanol as a function of [BQ]. Insert: $1/k_{1st}^{obs}$ vs. 1/[BQ].

In high viscosity solvents such as 1-BuOH, the relation of k_{1st}^{obs} versus [BQ] shows a negative curvature as shown in Fig. 6, which is the evidence [48,49] for the formation of triplet exciplex Eq. (5)[8,11,50–52].

$$^3(RB^{2-})^* + BQ \underset{k_{-a}}{\overset{k_a}{\rightleftarrows}} {}^3[(RB^{2-})^{\delta+}\cdots BQ^{\delta-}]^*$$
$$\xrightarrow{k_d} (RB^{2-})^{\bullet+} + BQ^{\bullet-}, \quad K = \frac{k_a}{k_{-a}} \tag{5}$$

The Eq. (6) can be derived from the Eq. (5) as follows [50].

$$\frac{1}{k_{1st}^{obs}} = \frac{1}{k_d} + \frac{1}{Kk_d[BQ]} \tag{6}$$

On applying Eq. (6), k_d can be evaluated from the intercept of the reciprocal plot (inset in Fig. 6) to be 3.0×10^7 s^{-1} from the slope, $K = k_a/k_{-a}$ was evaluated to be 65 M^{-1}. From the slope in the low concentration region showing linearity in Fig. 6, k_q can be obtained to be 1.7×10^7 M^{-1} s^{-1}, which is predicted to be equal to Kk_d at low [BQ] region. The K_{-a} value is calculated to be $2.6 \times 10^7 s^{-1}$ on assuming $k_q = k_a$ in high viscosity solvents. Thus, k_q is almost equal to Kk_d ($=1.9 \times 10^9$ M^{-1} s^{-1}). This implies that at low concentration region of [BQ], the electron transfer via exciplex is the rate-determining step, while at high concentration region of [BQ], dissociation processes of exciplex become rate-determining step.

In low viscosity solvents such as acetone, the pseudo-first-order decay rate constants show almost a linear relationship with BQ concentration. This may be due to the large values of k_d and k_{-a} leading low efficiency of exciplex formation in low viscosity solvents.

3.5. Electron transfer from donor

On addition of an electron donor such as 3,3′,5,5′-tetramethylbenzidine (TMB), the quenching of $^3(RB^{2-})^*$ was observed with the appearance of $TMB^{\bullet +}$ at 880 nm.

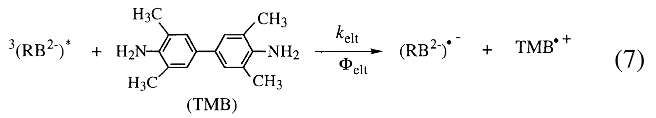

(7)

From the initial absorbance of $^3(RB^{2-})^*$, maximal absorbance of $TMB^{\bullet +}$, and their ϵ values, the quantum yield of the electron transfer (Φ_{elt}) can be evaluated as 0.24 in EtOH. The k_{elt} values can be evaluated by multiplying the quenching rate constants (k_q) for these reactions with Φ_{elt}. The k_q values summarized in Table 2 represent the maximal value of k_{elt} in each solvent. The k_q values are lower than the k_{diff} values and seem to be independent of viscosity of solvent (Table 2); this implies that the k_{elt} values are far less than k_{diff}. Although the plot of log k_q versus log η shows a few scattered points, the value of α was found to be 0.2 which was much lower than that of k_{diff}. The k_q values depend on ΔG^0 values; ΔG^0 values (−0.12 eV in benzonitrile) are less negative, which predicts $k_q < k_{diff}$. The possibility to form the exciplex between TMB and $^3(RB^{2-})^*$ may be low.

3.6. H-abstraction reactions

By the laser photolysis of RB^{2-} in the presence of 1,4-hydroquinone (HQ), an absorption band appeared at 405 nm with the decay of $^3(RB^{2-})^*$. The 405 nm band can be assigned to $HOC_6H_4O^{\bullet}$, [53] suggesting that H-atom abstraction reaction by $^3(RB^{2-})^*$ takes place. The rate constants (k_H) with substituted phenols as typical H-atom donors in three different solvents are summarized in Table 3. It is notable that α-tocopherol is highly reactive with $^3(RB^{2-})^*$ compared with phenol. For each H-atom donor, the k_H values increase according to the order: water > - ethanol ~ THF (Table 3).

The H-abstraction reactivity of $^3(RB^{2-})^*$ decreases with a decrease in the electron-donor ability of X in $4\text{-}XC_6H_4OH$. Similar substituent effects of phenol derivatives were reported for the reaction of safranine-T [54]. To investigate the solvent effect on the substituent effect, the Hammett plots of log k_H against σ^+-constants for the reactions of $^3(RB^{2-})^*$ with $4\text{-}XC_6H_4O\text{-}H$ according to Eq. (8) are shown in Fig. 7 in three different solvents.

$$\Delta(\log k_H) = \rho^+\sigma^+ \quad (8)$$

Although the k_H values for para-substituted phenols were also found to be higher compared to meta-substituted phenols (Table 3), the latter deviates from the lines connecting para-substituted phenols in the Hammett plots. In water, the k_H values for X = $-NH_2$, –OH, and $-OCH_3$ are similarly close to k_{diff} in water (= 4.5×10^9 M^{-1} s^{-1}), reaching an upper limit. The negative slopes (ρ^+) of the Hammett relation indicate the electrophilic nature of the reaction center of $^3(RB^{2-})^*$ with respect to $4\text{-}XC_6H_4OH$ [55,56]. The ρ^+ values were evaluated to be −5.0 in water, −4.2 in ethanol and −3.8 in THF, which indicates that the electrophilic nature of $^3(RB^{2-})^*$ increase with solvent polarity. Since the H-atom abstraction reaction is considered to occur at >C=O of RB^{2-}, the electrophilic nature of $^3(RB^{2-})^*$ suggests that the triplet state of >C=O behaves as $>C^{\bullet}\text{–}O^{\bullet}$ in which O atom is electron deficient. Negative ρ^+ values for $^3(RB^{2-})^*$ is larger than those of eosine (−3.6 in ethanol) and erythrosine (−3.7 in ethanol) [25], suggesting the high electrophilic nature of $^3(RB^{2-})^*$. The large negative ρ^+ values suggest that the transition state is quite polar; i.e., as shown in Eq. (9), the contribution of the electron (charge)-transfer character to the transition state is very large.

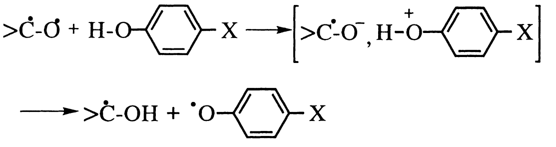

(9)

It is notable that although the H-abstraction reactions from thiophenols were observed for the triplet states of

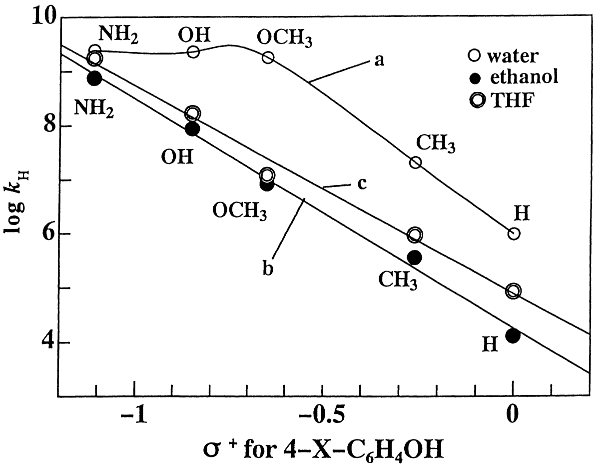

Fig. 7. Hammett plots of log k_H vs. σ^+-constants of $4\text{-}XC_6H_4OH$ for the reactions with $^3(RB^{2-})^*$ in (a) water, (b) ethanol and (c) THF.

Table 3
Second-order rate constants for the quenching of $^3(RB^{2-})^*$ with H-atom donors (k_H) in ethanol

H-atom donors	σ^+	k_H[a] (M^{-1} s^{-1}) Water	Ethanol	THF
4-aminophenol	−1.11	2.5×10^9	7.7×10^8	1.8×10^9
3-aminophenol	−0.16	2.4×10^9	6.7×10^7	3.5×10^7
1,4-hydroquinone	−0.85	2.3×10^9	8.8×10^7	1.7×10^8
4-methoxyphenol	−0.65	1.8×10^9	8.3×10^6	8.7×10^6
3-methoxyphenol	0.05	2.2×10^7	6.2×10^5	1.1×10^6
4-methylphenol	−0.26	2.0×10^7	3.6×10^5	9.3×10^5
Phenol	0	9.6×10^5	1.3×10^4	8.6×10^4
α-tocopherol		–[b]	1.5×10^8	1.6×10^8

[a] For other derivatives, the rate constants can be estimated from the plots in Fig. 7.

[b] α-tocopherol is not soluble in water.

Table 4
Second-order rate constants (k_H) for the quenching of $^3(RB^{2-})^*$ with hydroquinone (HQ) and 4-MeOC$_6$H$_4$OH in water-THF and AN-THF mixtures

THF %	k_H (M^{-1} s^{-1})		
	4-MeOC$_6$H$_4$OH	HQ	
	water-THF	water-THF	AN-THF
0	1.8×10^9	2.3×10^9	1.1×10^9
20	8.4×10^8	8.1×10^8	2.5×10^8
40	2.2×10^8	2.6×10^8	1.9×10^8
60	2.5×10^7	1.2×10^8	1.3×10^8
80	1.5×10^7	9.9×10^7	9.9×10^7
100	8.7×10^6	1.7×10^8	1.7×10^8

eosine and erythrosine [25], $^3(RB^{2-})^*$ do not show reactivity to thiols.

Solvent mixture effects were observed in the k_H values for the reactions of $^3(RB^{2-})^*$ with 4-methoxyphenol and hydroquinone, when the reactions were performed in water-THF mixture and acetonitrile(AN)-THF mixture (Table 4). The log k_Hs are plotted against THF fraction as shown in Fig. 8. The k_H values decrease with addition of THF in the mixtures due to the decrease in polarity. In the case of 4-methoxyphenol, the variation of log k_H with THF in water-THF mixture shows almost a linear relationship according to the dielectric constant change of the mixture (Fig. 8), which implies that the solvent composition in the bulk solution is same as that of the solvation shell surrounding the reactants [4-methoxyphenol and $^3(RB^{2-})^*$]. On the other hand, a downward deviation from the linear line **a** is shown for HQ (Fig. 8), which suggests that THF-fraction in the solvation shell surrounding the reactants [HQ and $^3(RB^{2-})^*$] is higher than the bulk composition. In the case of AN-THF mixture, polar AN in the solvation shell surrounding the reactants is easily expelled only by the addition of ca. 20% THF.

4. Conclusions

The T–T absorption band of RB^{2-} in the near-IR region, where the absorption and emission of RB^{2-} do not disturb, was quite convenient to follow many kinds of reactions of $^3(RB^{2-})^*$ in various solvents. In the electron transfer reaction with BQ, the exciplex formation was confirmed by BQ-concentration effect in high viscosity solvent. Hammett plots of H-atom abstraction reaction indicates the electrophilic nature of the reaction center of $^3(RB^{2-})^*$, which is higher than those of eosine and erythrosine. Solvent mixture also affects the reaction rates, revealing that the solvation shell of polar solvent surrounding the reactants is destroyed by nonpolar solvent. Thus, substituent effects and solvent effects based on the rate constants obtained from the direct observation of $^3(RB^{2-})^*$ in the near-IR region afford a lot of useful information about reaction processes.

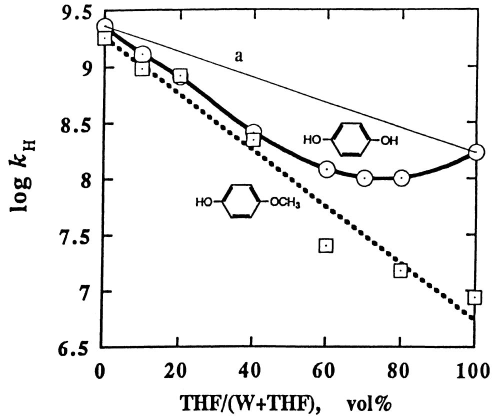

Fig. 8. Log k_H vs. THF fraction in water–THF for $^3(RB^{2-})^*$/4-MeOC$_6$H$_4$-OH and $^3(RB^{2-})^*$/HOC$_6$H$_4$-OH system.

References

[1] S. Kato, T. Watanabe, S. Nagaki, M. Koizumi, Bull. Chem. Soc. Jpn. 33 (1960) 262.
[2] Y. Usui, K. Itoh, M. Koizumi, Bull. Chem. Soc. Jpn. 38 (1965) 1015.
[3] T. Ohno, Y. Usui, M. Koizumi, Bull. Chem. Soc. Jpn. 38 (1965) 1022.
[4] K. Kikuchi, H. Kokuban, M. Koizumi, Bull. Chem. Soc. Jpn. 44 (1971) 1527.
[5] A.W.-H. Mau, O. Johansen, W.H.F. Sasse, Photochem. Photobiol. 41 (1985) 503.
[6] Y. Usui, H. Misaw, H. Sakuragi, K. Tokumaru, Bull. Chem. Soc. Jpn. 61 (1988) 3335.
[7] S.M. Linden, D.C. Neckers, J. Am. Chem. Soc. 110 (1988) 1257.
[8] E.S. Klimtchuk, G. Irinyi, I.V. Khudyakov, L.A. Margulis, V.A. Kuzmin, J. Chem. Soc. Faraday Trans. I 85 (1989) 4119.
[9] A. Katsuki, K. Akiyama, S. Tero-Kubota, Bull. Chem. Soc. Jpn. 68 (1995) 3383.
[10] P. Douglas, G. Waechter, A. Mills, Photochem. Photobiol. 52 (1990) 473.
[11] C.R. Lambert, I.E. Kochevar, Photochem. Photobiol. 66 (1997) 15.
[12] G. Bottiroli, A.C. Croce, P. Balzarini, D. Locatelli, P. Baglioni, P.L. Nostro, M. Monici, R. Prates, Photochem. Photobiol. 66 (1997) 374.
[13] T.P. Sarathy, P. Srinivas, K.N. Rao, B. Sethuram, T.N. Rao, J. Macromol. Sci. Chem. A 26 (1989) 1347.
[14] T. Tani, S. Kikuchi, K. Honda, Photogr. Sci. Eng. 12 (1968) 80.
[15] F. Rizzuto, J.D. Spikes, Photochem. Photobiol. 25 (1977) 465.
[16] T. Shen, Z.-G. Zhao, Q. Yu, H.-J. Xu, J. Photochem. Photobiol. A: Chem. 47 (1989) 203.
[17] E. Chesneau, D.C. Neckers, J. Photochem. Photobiol. A: Chem. 42 (1988) 269.
[18] T. Sarna, J. Zajac, M.K. Bowman, T.G. Truscott, J. Photochem. Photobiol. A: Chem. 60 (1991) 295.
[19] A. Mills, C. Lawrence, P. Douglas, J. Chem. Soc., Faraday Trans. 2(82) (1986) 2291.
[20] L.I. Grossweiner, E.F. Zwicker, J. Chem. Phys. 34 (1961) 1411.
[21] R. Gerdes, D. Wohrle, W. Spiller, G. Schneider, G. Schnurpfeil, G. Ekioff Schulz, J. Photochem. Photobiol. A: Chem. 3 (1997) 65.
[22] N.J. Turro, Modern Molecular Photochemistry, Benjamin/Cummings, Menlo Park. CA, 1978.
[23] P.J. Wagner, R.J. Truman, J.S. Scaiano, J. Am. Chem. Soc. 107 (1985) 7093.
[24] S.E. Braslavsky, G.E. Heibel, Chem. Rev. 92 (1992) 1381.
[25] S.D.-M. Islam, Y. Yoshikawa, M. Fujitsuka, A. Watanabe, O. Ito, Bull. Chem. Soc. Jpn. 71 (1998) 1543.
[26] P. Bilski, A.S.W. Li, C.F. Chignell, Photochem. Photobiol. 54 (1991) 345.

[27] M. Rozanowska, I. Ciszewska, W. Korytowski, T. Sama, J. Photochem. Photobiol. B 29 (1995) 71.

[28] V. Wintgens, J.C. Scaiano, S.M. Linden, D.C. Neckers, J. Org. Chem. 54 (1989) 5242.

[29] A. Watanabe, O. Ito, J. Phys. Chem. 98 (1994) 7736.

[30] O. Valdes-Aguilera, D.C. Neckers, J. Phys. Chem. 92 (1988) 4287.

[31] D.H. Volman, G.S. Hammond, D.C. Neckers, Advanced in Photochemistry, vol. 18, Wiley, New York, 1993, p. 357.

[32] R. Lochet, C.C.R. Nouchi, Seances Acad. Sci. 260 (1965) 1897.

[33] C.V. Zakharova, A.K. Chibisov, Khim. Vys. Energy 18 (1984) 552.

[34] A. Jodlbauer, H.V. Tappeiner, Arch. Klin. Med. 82 (1905) 520.

[35] H.V. Tappeiner, Arch. Klin. Med. 86 (1906) 478.

[36] V.S. Srinivasan, D. Podoiski, N. Westric, D.C. Neckers, J. Am. Chem. Soc. 100 (1978) 6513.

[37] Y. Usui, Chem. Lett. (1973) 743.

[38] D.H. Volman, C.S. Hammond, D.C. Neckers, Advanced in Photochemistry, vol. 18, Wiley, New York, 1993, p. 358.

[39] P.B. Merkel, D.R. Keams, J. Am. Chem. Soc. 94 (1972) 1029.

[40] H.-J. Timpe, S. Neuenfeld, J. Chem. Soc. Faraday Trans. 88 (1992) 2329.

[41] H.-J. Timpe, K.-P. Kronfeld, U. Lammel, J. Photochem. Photobiol. A: Chem. 52 (1990) 111.

[42] G.J. Kavarnos, N.J. Turro, Chem. Rev. 86 (1986) 422.

[43] G. Amirzadeh, W. Schnabel, Macromol. Chem. 182 (1981) 2821.

[44] T. Shida, Electronic Absorption Spectra of Radical Ions, Elsevier, Amsterdam, 1988.

[45] S. Hirayama, H. Yasuda, A.D. Scully, M. Okamoto, J. Phys. Chem. 98 (1994) 4609, and references cited therein.

[46] J.B. Birks, Photophysics of Aromatic Molecules, Interscience, New York, 1970, p. 497.

[47] D. Rehm, A. Weller, Isr. J. Chem. 8 (1970) 259.

[48] H. Shizuka, H. Hagiwara, M. Fukushima, J. Am. Chem. Soc. 107 (1985) 7816.

[49] T. Kiyota, M. Yamaji, H. Shizuka, J. Phys. Chem. 100 (1996) 672.

[50] R. Rathore, S.M. Hubig, J.K. Kochi, J. Am. Chem. Soc. 119 (1997) 11468.

[51] Y. Usui, H. Misawa, H. Sakuragi, K. Tokumaru, Bull. Chem. Soc. Jpn. 60 (1987) 1573.

[52] Y. Nishimura, H. Sakuragi, K. Tokumaru, Bull. Chem. Soc. Jpn. 65 (1992) 2887.

[53] G.E. Adams, B.D. Michael, Trans. Faraday Soc. 63 (1967) 1171.

[54] M.C. Neumann, I.A. Pastre, C.M. Previtali, J. Photochem. Photobiol. Photobiol. A: Chem. 61 (1991) 91.

[55] A.J. Gordon, R.A. Ford, The Chemist's Companion, Wiley, New York, 1972, p. 145.

[56] O. Ito, Res. Chem. Intermed. 21 (1995) 69.